

DOI: 10.1070/QE2016v046n01ABEH015591

Analysis of the effects of mismatched errors on coherent beam combining based on a self-imaging waveguide

R. Tao, X. Wang, P. Zhou, L. Si

Abstract. **A theoretical model of coherent beam combining (CBC) based on a self-imaging waveguide (SIW) is built and the effects of mismatched errors on SIW-based CBC are simulated and analysed numerically. With the combination of the theoretical model and the finite difference beam propagation method, two main categories of errors, assembly and nonassembly errors, are numerically studied to investigate their effect on the beam quality by using the M^2 factor. The optimisation of the SIW and error control principle of the system is briefly discussed. The generalised methodology offers a good reference for investigating waveguide-based high-power coherent combining of fibre lasers in a comprehensive way.**

Keywords: *self-imaging effects, laser beam combining, fibre lasers.*

1. Introduction

Since the first demonstration of self-imaging in a waveguide [1], a multimode waveguide based on self-imaging effects has become an important device to split and combine multiple optical beams [2], which is an important function in integrated optics. Due to excellent properties (compact size, low loss, stable splitting ratio) and ease of fabrication (good fabrication tolerances), multimode interference couplers based on a self-imaging waveguide (SIW) have been fabricated and incorporated into more complex photonic integrated circuits for optical communication, i.e., lasers/amplifiers [3, 4], polarisation-insensitive Mach–Zehnder interferometers (MZI) switches [5–6], polarisation diversity receivers [7] and optical hybrids for phase diversity networks [8, 9]. Recently, Christensen et al. [10] have developed for the first time SIWs to realise coherent beam combining (CBC) and Uberna et al. [11] have experimentally realised CBC of SIW-based fibre lasers under medium power levels. CBC based on a SIW can provide much better combining efficiencies and eliminate side lobes in the far field [11]. These SIW-based CBC properties make this approach more promising as compared with the previous free-space phased array architectures, which is the prevalent architecture for CBC [12–19]. We have derived the analytical expression for self-imaging properties of SIWs and have simulated the properties by finite difference beam propagation method (FDBPM), which shows that SIW-based CBC allows one to obtain a combined laser beam without side lobes and with near-diffraction-limited beam quality [20, 21]. Due to the aforementioned advantage, SIW-based CBC is one of the promising approaches to scale fibre lasers to a higher power with an excellent beam quality.

The compact structure is one of the advantages of a waveguide device, which results in a high degree of assemblage and operation accuracy of CBC systems based on SIWs. However, the aforementioned merit also leads to the fact that SIW-based CBC inevitably experiences many kinds of mismatched errors that are unique from those of free-space phased array architectures [13]. The beam quality of a coherently combined beam degrades due to these errors. We classify these errors into two main categories. The first one is assembly errors which are introduced by implementation of SIW-based CBC, including the array offset error (the axis of the SIW and fibre laser array are parallel to each other but are not aligned), array pointing error (the axis of the SIW cannot be exactly parallel to that of the fibre laser array), beam position error (the incident positions at the SIW are not always exactly matched with the self-imaging position) and beam pointing error (the axis of the fibre laser in the array cannot be exactly parallel). The other category is nonassembly errors which are introduced by the fibre laser. Phase errors (phase differences between beamlets due to the performance of the phase controlling system), power fluctuation (the fluctuation of the output power of the fibre laser) and beam size error (the beam size of the fibre laser cannot be exact the same) fall into this category. The effects of mismatched errors on coherently combined fibre laser beams based on free-space phased arrays have been studied in Refs [13, 22–24]. In our previous study, the self-imaging properties of SIWs have been derived analytically and the feasibility of SIW-based CBC has been studied numerically. The principle for the waveguide optimisation has been briefly discussed and some handy design rules have been obtained [20, 21]. However, to the best of our knowledge, the effects of mismatched errors on SIW-based CBC have not been investigated in detail.

In the present paper, we have studied analytically SIW-based CBC of fibre lasers by using the mode-decomposition theory and have employed the FDBPM to verify numerically the analytical derivation. Based on the combination of the analytical results and FDBPM, we have analysed the effects of the assembly and nonassembly errors on the beam quality of a coherently combined fibre laser beam numerically with some instructive discussion.

2. Theoretical model

The system configuration of SIW-based CBC has been presented in our earlier work [20, 21] and, therefore, we do not

R. Tao, X. Wang, P. Zhou, L. Si College of Optoelectric Science and Engineering, National University of Defense Technology, Changsha, Hunan 410073, China; e-mail: zhoupu203@@163.com

Received 21 June 2014; revision received 5 November 2014
Kvantovaya Elektronika **46** (1) 61–67 (2016)
Submitted in English

describe it here to save place. The theory has been developed for a two-dimensional case. However, the presented results are also relevant for square and rectangular self-imaging produced by waveguides having square or rectangular cross sections [25, 26]. If we denote the input field of a single beam by $f(x)$, then the total input field distribution of a phase-locked laser array can be written as

$$f_{\text{in}}(x) = C\left[\frac{1}{C}\sum_{q=0}^{N-1} f(x - x_q)\exp(-\text{j}\varphi_q)\right], \tag{1}$$

where

$$C = \exp(-\text{j}\beta_0 L_N^M)\sum_{q=0}^{N-1}\exp\left(-\text{j}\pi\frac{x_q}{W} - \text{j}\varphi_q\right), \tag{2a}$$

$$x_q = (2q + 1 - N)\frac{M}{N}\frac{W}{2}, \tag{2b}$$

$$\varphi_q = q(N - q - 1)\frac{M}{N}\pi. \tag{2c}$$

Here, x_q is the beam position at the input; φ_q is the piston phase, which is necessary to realise coherent combining and introduced by a control mechanism, i.e. a phase modulator; N is the number of fibre lasers; M together with N define possible waveguide lengths L_N^M, which is due to the presence of several positions in the waveguide where self-imaging can be achieved (in addition, M and N are any positive integers without a common divisor); and W is the active waveguide diameter (Fig. 1) equal to the physical thickness W_0, which is slightly corrected at both sides by the Goos–Hahnchen penetration depth in the cladding having a refractive index $n_{\text{cl}} < n$ [25–27].

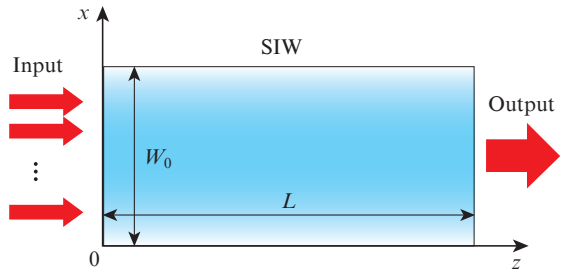

Figure 1. Schematic diagram of a waveguide.

For a fibre laser,

$$f(x) = \left(\frac{1}{\pi}\right)^{1/4}\sqrt{P/w}\exp(-x^2/w^2), \tag{3}$$

where P is the power of the fibre laser and w is the beam radius.

The strongly guided eigenmodes for the SIW have the form [26]

$$E_i(x) = \sin\left[\pi(i + 1)\frac{x}{W}\right], \tag{4}$$

where $i = 0, 1, 2, \ldots$ is the mode number.

Using a spatial Fourier decomposition, the field distribution $f(x)$ can be written as a superposition of the infinite number of strongly guided even eigenmodes $E_i(x)$ with the coefficients a_i:

$$f(x) = \sum_{i=0}^{\infty} a_{2i}E_{2i}(x), \quad a_i = \frac{2}{W}\int_0^W f(x)E_i^*(x)\,\text{d}x. \tag{5}$$

Equations (5) were obtained by using the symmetry properties of the input light distribution and the axially aligned incident light properties (the direction of incidence for the input light field is parallel to the z axis). Then

$$f_{\text{in}}(x) = C\left\{\sum_{i=0}^{\infty} a_{2i}\left[\frac{1}{C}\sum_{q=0}^{N-1} E_{2i}(x - x_q)\exp(-\text{j}\varphi_q)\right]\right\}. \tag{6}$$

Using

$$\frac{1}{C}\sum_{q=0}^{N-1} E_{2i}(x - x_q)\exp(-\text{j}\varphi_q) = B_{2i}E_{2i}(x), \tag{7}$$

where

$$B_{2i} = \frac{1}{C}\sum_{q=0}^{N-1}\exp\left[-\text{j}\pi(2i + 1)\frac{x_q}{W} - \text{j}\varphi_q\right], \tag{8a}$$

and replacing the summation index q of the sum by $N - q - 1$, expression (8a) can be written as

$$B_{2i} = \frac{1}{C}\sum_{q=0}^{N-1}\exp\left[\text{j}\pi(2i + 1)\frac{x_q}{W} - \text{j}\varphi_q\right]. \tag{8b}$$

We introduce the coefficients A_{2i}, which are defined as

$$A_0 = \exp(\text{j}\beta_0 L_N^M), \quad A_{2i} = A_{2(i-1)}\exp[-\text{j}\pi(M/N)2i]. \tag{9}$$

According to Eqns (2a) and (8), we have $A_0 = B_0$. Using Eqns (2b), (2c) and (8a), we can obtain

$$\Phi_{2i,\text{q}-1} = \Phi_{2(i-1),q} + \pi(M/N)(-2i). \tag{10}$$

Recalling the N periodicity of the summands, we have

$$B_{2i} = B_{2(i-1)}\exp[-\text{j}\pi(M/N)2i]. \tag{11}$$

According to Eqns (9) and (11), the following relationship is established:

$$A_{2i} = B_{2i}. \tag{12}$$

With Eqn (12) taken into account, Eqn (6) can be expressed as

$$f_{\text{in}}(x) = C\sum_{i=0}^{\infty} a_{2i}A_{2i}E_{2i}(x). \tag{13}$$

In Eqn (4), the transverse propagation constants are

$$k_{xi} = (i + 1)\pi/W. \tag{14}$$

The corresponding longitudinal propagation constants are

$$\beta_i^2 = n_2 k_0^2 - k_{xi}^2. \tag{15}$$

Using the paraxial approximation, one can obtain

$$\beta_i \approx nk_0 - k_{xi}^2/2nk_0 . \quad (16a)$$

$$\beta_i \approx nk_0 - \Delta\beta_{02}/8,\ \ \Delta\beta_{02} = \beta_0 - \beta_2 \approx 4\pi^2/(nk_0W^2), \quad (16b)$$

$$\beta_{2i} \approx \beta_0 - i(i+1)\Delta\beta_{02}/2, \quad (16c)$$

where $k_0 = 2\pi/\lambda$ is the propagation constant in vacuum.

If the waveguide length

$$L_N^M = \frac{M}{N}2L_c = \frac{M}{N}\frac{2\pi}{\Delta\beta_{02}}, \quad (17)$$

where $L_c = \pi/\Delta\beta_{02}$ is the coupling length between two lowest-order modes, then the output field is:

$$f_{out}(x) = C\sum_{i=0}^{\infty} a_{2i}A_{2i}E_{2i}(x)\exp(-j\beta_{2i}L_N^M) = Cf(x). \quad (18)$$

One can see from Eqn (18) that $f(x)$ at different position numbered by $q = 0, 1, \ldots, N-1$ are combined into one common sum, which means that SIW-based CBC has been achieved.

3. Numerical calculations

To study the formulas derived in Section 2 numerically, we use the FDBPM [28,29] with 'transparent' boundary conditions [30,31] to simulate the light propagation in the planar waveguide section, which is the same as that in Refs [20,21]. We consider a planar waveguide with $W = 50$ μm and $n = 1.45$. The waveguide is in the air, i.e., $n_{cl} = 1.00$. We also assume that $\lambda = 1.00$ μm. In combining two fibre lasers ($N = 2$, $M = 1$), we have $L_2^1 = 1833.5$ μm from Eqns (3) and (18). As shown in Fig. 2, two equal-power Gaussian beams with a waist diameter of 5 μm are launched vertically into the waveguide at $z = 0$. The relative piston phase of two input fields is given by Eqn (2c). In our FDBPM simulation, we choose the discretisation sizes $x = 0.02$ μm. The field distribution of light in the waveguide is shown in Fig. 2, which indicates that the fibre lasers are coherently combined into a single beam.

Before we study the effects of the aberration, we have to find the optimal operation conditions, which result in optimal combining and can be used for the evaluation of the effects of mismatched errors. The parameter M^2 is taken as a characteristic parameter to analyse the combining performance of the system. Figure 3 presents the dependence of the beam quality M^2 on the waveguide length and the transverse intensity distribution of light. The optimal waveguide length, which is 1834.5 μm corresponding to $M^2 = 1.156$, differs from the calculated length, which is 1833.5 μm corresponding to $M^2 = 1.157$. However, the relative length error is about 0.05% and the degradation of the beam quality is about 0.08%. The relative length error and the degradation of the beam quality are negligibly small, which indicates that the formulas in Section 2 are accurate enough.

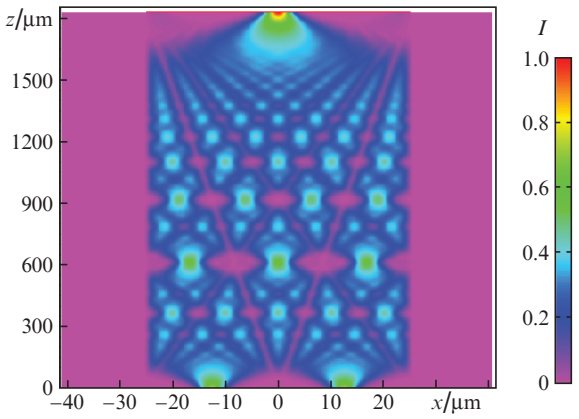

Figure 2. Distribution of the light field.

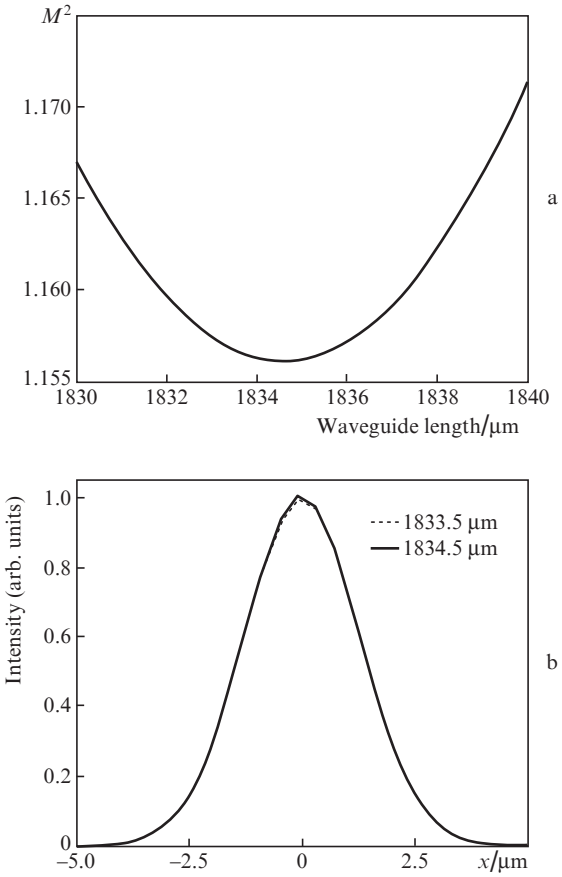

Figure 3. (a) Beam quality M^2 as a function of the waveguide length and (b) output intensity distribution.

In the following simulation, the length of the waveguide is fixed and equal to the optimal waveguide length, which is 1834.5 μm for the case considered here. We define the fill factor as $t_{fill} = 2w/(W/N)$. Figure 4 shows the dependence of M^2 on t_{fill}. The optimal fill factor is 0.52, which corresponds to an optimal waist of 13 μm. It can be observed that the curve has a 'U'-type profile and, when $0.4 < t_{fill} < 0.6$, the parameter M^2 is virtually independent of the fill factor and a diffraction-limited beam can be produced.

3.1. Effects of mismatched errors

The primary requirement for highly efficient coherent combining of fibre lasers based on a SIW is that individual lasers must be virtually identical to allow perfectly reverse self-

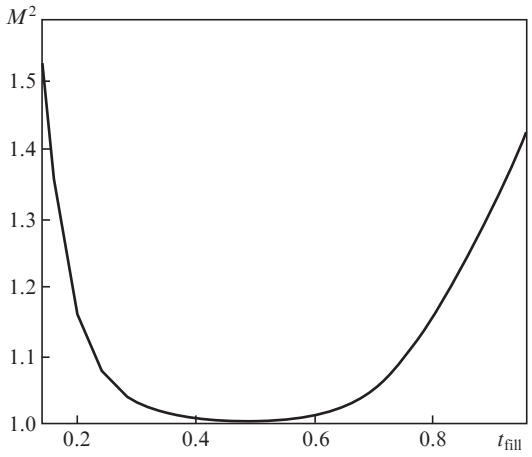

Figure 4. Beam quality parameter M^2 vs. the fill factor.

imaging. This means that the lasers must be spatially matched and co-aligned, as well as locked in phase with high precision. However, these conditions are hard to be perfectly met in practical applications, which leads to a decrease in the combining efficiency. Figures 5 and 6 show near-field intensity distributions of laser light without any errors and with errors, respectively. In the first case (Fig. 5), a single beam without any side-lobes is produced. However, with mismatched errors (piston phase errors among each laser beam, offset errors and pointing errors) there appear some side-lobes besides the main-lobe (Fig. 6). Therefore, the errors cause the beam quality degradation and, therefore, it is important to study the effects of various aberrations to get a detailed result.

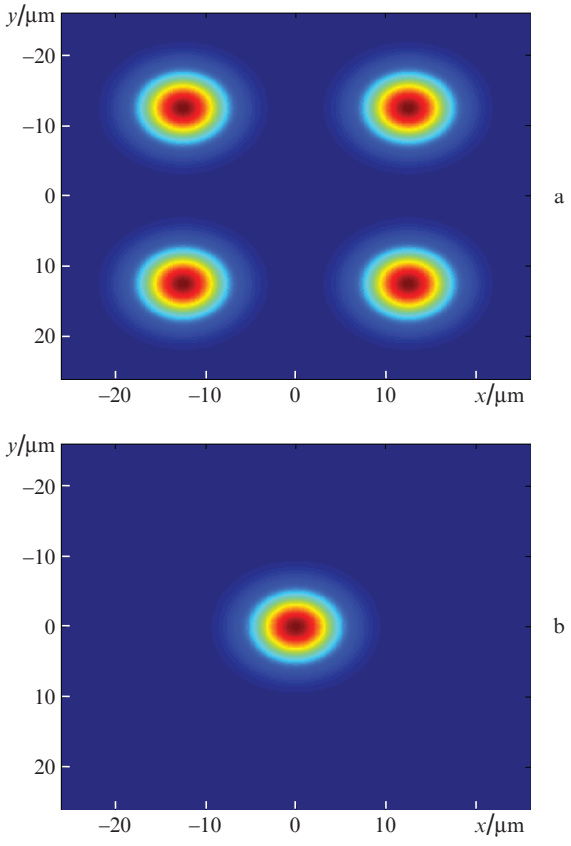

Figure 5. (a) Input and (b) output intensity distributions without aberrations.

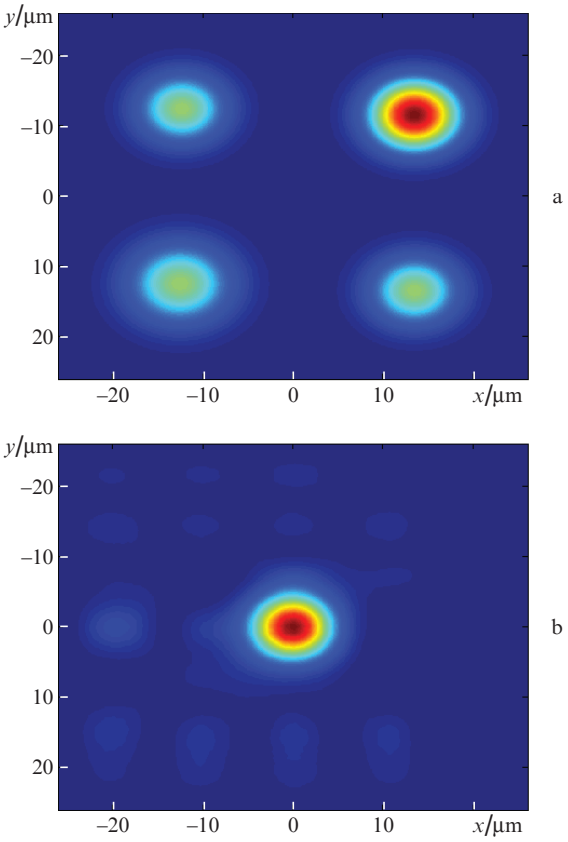

Figure 6. (a) Input and (b) output intensity distributions with aberrations.

Uberna et. al. [11] experimentally demonstrated a combined 2×2 fibre laser array in a two-dimensional SIW. This fibre laser array can be taken as an initial unit to scale to more fibre lasers in accordance with the cascaded configuration (Fig. 7). Therefore, we mainly focus our attention on analysis of a 2×2 fibre laser array.

To study the effects of the aberration on a combined laser beam, use is made of the optimal parameters of the waveguide: the waveguide length is 1834.5 μm and the Gaussian beams with a waist $2w_{opt}$ = 13 μm (t_{fill} = 0.52) are launched vertically in the $z = 0$ plane. We define a tolerance on the error

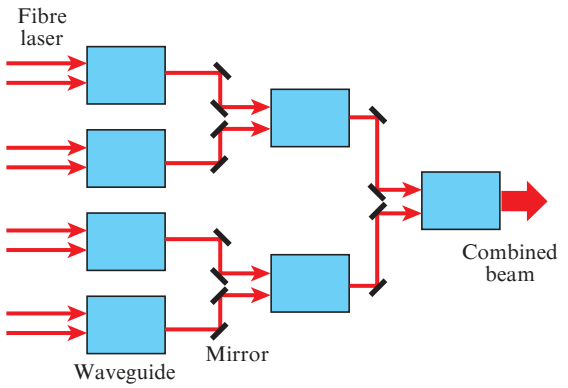

Figure 7. Cascaded arrangement of the waveguide.

to ensure $M^2 < 1.2$. In the presence of mismatched errors, according Eqn (3), the field of the input fibre laser array can be written as

$$f_{\text{in}}(x) = \left(\frac{1}{\pi}\right)^{1/4} \sum_{q=0}^{N-1} \sqrt{\frac{P + \delta P_q}{w_{\text{opt}} + \delta w_q}} \exp[-\text{j}(\varphi_q + \delta\varphi_q)] \times$$

$$\times \exp\left[-\frac{(x\cos(\delta\theta_q) - x_q - \delta x_q)^2}{(w_{\text{opt}} + \delta w_q)^2}\right], \qquad (19)$$

where δP_q, δw_q, $\delta\theta_q$, δx_q and $\delta\varphi_q$ denote the variation in power, beam radius, pointing, position and residual piston phase of the qth laser beam.

3.1.1. Effects of the assembly factors. There are mainly four kinds of assembly errors: array offset error, array pointing error, beam position error and beam pointing error. Limited by the precision of machining and assembling, the symmetric axes of lasers emitted from a fibre laser array cannot strictly parallel to that of the waveguide, which is defined as the array offset error ($t_{\text{array}} = \delta x/W$, $\delta x_0 = ... = \delta x_{N-1} = \delta x$) and the array pointing error ($\delta\theta_0 = ... = \delta\theta_{N-1} = \delta\theta$). Figure 8 shows the variation of the beam quality as a function of the array offset error t_{array} and array pointing error $\delta\theta$. One can see that the M^2 value decreases proportionally to the mismatch between the array and the waveguide. The offset error and pointing error should be controlled within 0.02° and 0.5°, respectively (for $M^2 < 1.2$).

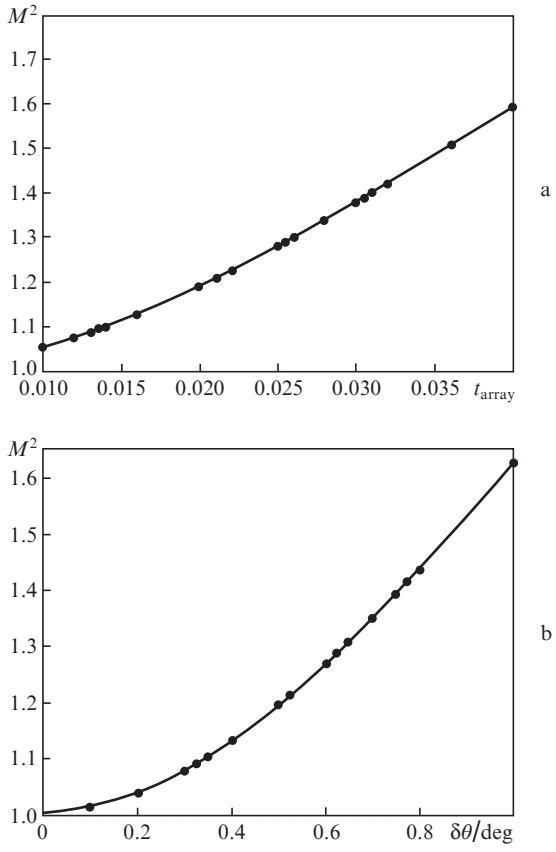

Figure 8. Beam quality M^2 as a function of (a) the array offset error and (b) array pointing error (points show the calculated data and the solid curve is the fitting curve).

In fact, the optical axes of lasers in an array cannot be strictly parallel to each other and the relative position of each laser beam cannot be strictly matched to the correct position on the waveguide, which is defined as the beam position error ($t_{\text{posit}} = \delta x_q/W$) and the beam pointing error ($\delta\theta_q$). Figure 9 presents the beam quality as a function of the beam position error and beam pointing error. One can see that for the condition $M^2 < 1.2$ to be fulfilled, the position error and pointing error of a single beam should be controlled within $-0.025 < t_{\text{posit}} < 0.021$ and $\delta\theta_q < 0.55°$, respectively.

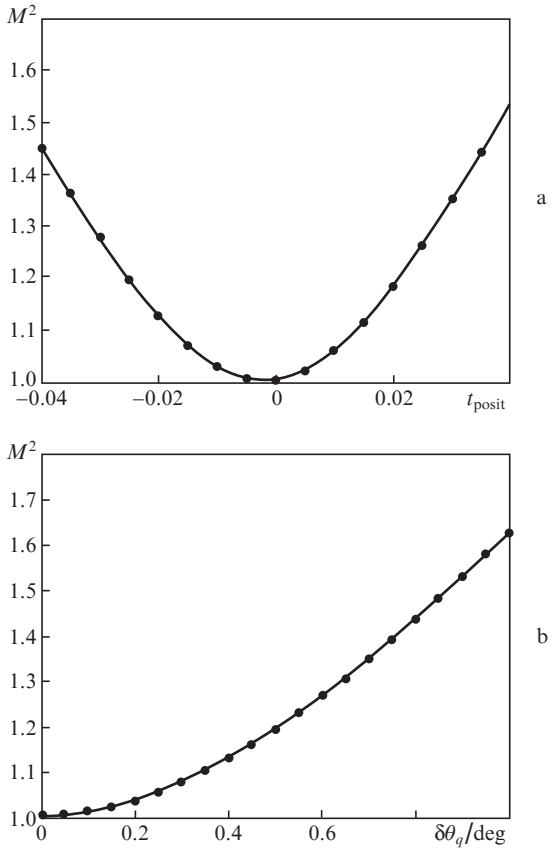

Figure 9. Beam quality M^2 as a function of (a) the beam position error and (b) beam pointing error (points show the calculated data and the solid curve is the fitting curve).

3.1.2. Effects of the nonassembly factor. There are mainly three kinds of nonassembly errors: piston phase error $\delta\varphi_q$, power fluctuation $t_P = \delta P_q/P$ and beam size error $t_{\text{b}} = \delta w_q/w_{\text{opt}}$ (Fig. 10). One can see that the beam quality of the combined laser beam depends on the aberrations of separate beams. To ensure a near-diffraction limited combined laser beam, the residual piston phase error must be controlled to within $\pi/10$, the fluctuation of the power must be less than 1 and the beam size error must lie in the range from –0.07 to 0.11.

The tolerances of mismatched errors are listed in Table 1, which shows that each kind of mismatched errors affects the beam quality of a coherently combined beam. However, in engineering practice, we think that the effect of several errors can be mitigated or eliminated by technical improvements. The power fluctuation and beam size error can be mitigated by improving the reliability of commercial fibre lasers. The array offset error and array pointing error can be mitigated by accurately adjusting the experimental platform and optimally

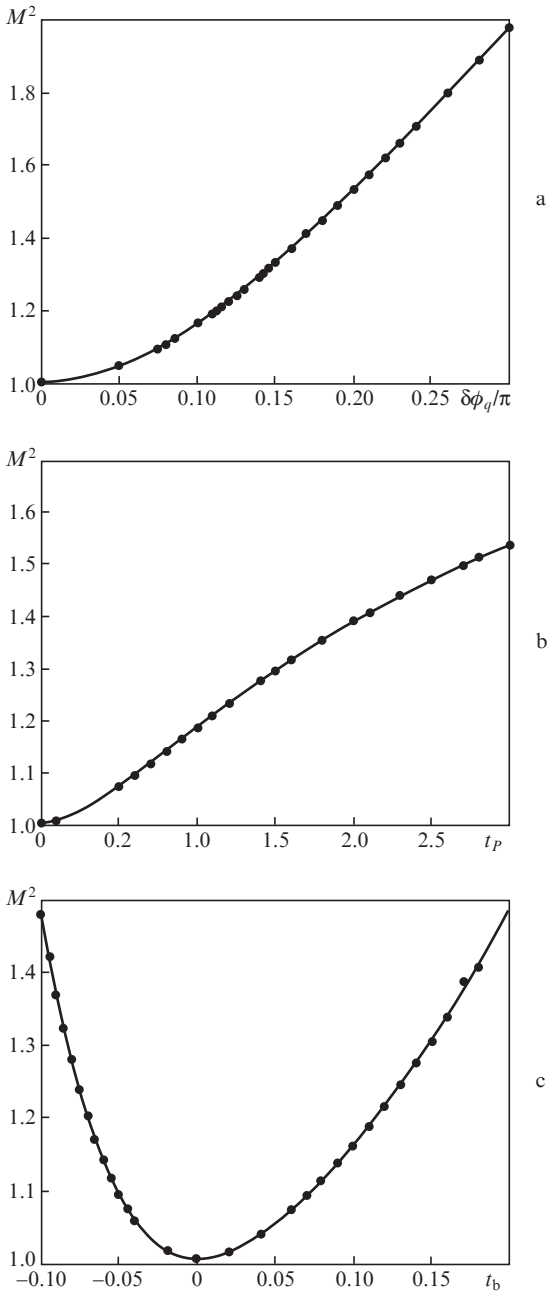

Figure 10. Beam quality M^2 as a function of (a) the piston phase error, (b) power fluctuations and (c) beam size error (points show the calculated data and the solid curve is the fitting curve).

Table 1. Tolerance of the aberrations.

Nonassembly factors	Tolerances
Residual piston phase error $\delta\varphi_q$	$< \pi/10$
Power fluctuation $t_P = \delta P_q/P$	< 1
Beam size error $t_b = \delta w_q/w_{opt}$	$-0.07 < t_b < 0.11$
Assembly factors	
Array offset error $t_{array} = \delta x/W$ $\delta x_0 = ... = \delta x_{N-1} = \delta x$	< 0.02
Array pointing error $\delta\theta_0 = ... = \delta\theta_{N-1} = \delta\theta$	$< 0.5°$
Beam position error $t_{posit} = \delta x_q/W$	$-0.025 < t_{posit} < 0.021$
Beam pointing error $\delta\theta_q$	$< 0.55°$

designing the experiment configuration. The position error and pointing error of a single fibre laser can be mitigated by precision assemblage of the fibre laser. Although the phase noise of the kilowatt-level fibre laser has been demonstrated to be eliminable experimentally [18], questions, such as the effects of the SIW on the phase characteristics and whether the phase noise of the CBC system based on a SIW can be mitigated, remain open and require a further investigation.

4. Conclusions

Coherent combining of fibre lasers based on a SIW offers an attractive method for obtaining a high-power laser with a good beam quality. The beam quality of the combined laser will be degraded due to aberrations. The theoretical model of SIW-based CBC is a setup based on mode-decomposition theory and the effects of aberrations on SIW-based CBC are simulated using the FDBPM. We categorise the aberrations into assembly and nonassembly factors, and propose a general methodology to study the effects of all the aberration factors.

By using the M^2 factor, we have shown that there exists an optimal beam width of the input fibre laser, with which we can achieve a diffraction-limited output laser beam (M^2 = 1.0054). Because the M^2 factor weakly changes, a diffraction-limited beam can be produced in the range $0.4 < t_{fill} < 0.6$. By investigating the effects of the aberrations using the analytical formulas and the FDBPM, it is found that for the condition $M^2 < 1.2$ to be fulfilled, the phase error must be controlled to within $\pi/10$, and the pointing error of the fibre array and of the single fibre laser should be less than 0.55° and 0.5°, respectively. One should also take into account that a slight array offset error or a slight beam position error induces a significant degradation of the beam quality; the influence of the power fluctuation and beam size error also should be considered.

Of all the aberrations, the effects of the power fluctuation, beam size error, offset error and pointing error of an array or a fibre laser in the array can be mitigated or eliminated by technical improvements, while the phase errors is still a challenge to the use of SIW-based coherent combining in engineering practice. Our methodology investigates the coherent combining of fibre laser beams in a more comprehensive way and the results can provide a reference for the designing of CBC of high-power SIW-based lasers.

Acknowledgements. This work was partially supported by the Innovation Foundation for Excellent Graduates of the National University of Defense Technology (Grant No. B120704) and Hunan Provincial Innovation Foundation For Postgraduates (Grant No. CX2012B035).

References

1. Bryngdahl O. *J. Opt. Soc. Am.*, **63**, 416 (1973).
2. Soldano L.B., Pennings E.C.M. *J. Lightwave Technol.*, **73**, 615 (1995).
3. Van Roijen R., Pennings E.C.M., van Stralen M.J.N., van Dongen T., Verbeek B.H., van der Keijden J.M.M. *Appl. Phys. Lett.*, **64**, 1753 (1994).
4. Baker H.J., Lee J.R., Hall D.R. *Opt. Express*, **10**, 297 (2002).
5. Zucker J.E., Jones K.L., Chiu T.H., Tell B., Brown Goebeler K. *J. Lightwave Technol.*, **10**, 1926 (1992).
6. Bachmann M., Smit M.K., Besse P.A., Gini E., Melchior H., Soldano L.B. *Proc. Opt. Fiber Conf. and Intern. Conf. on Integrated Optics and Optical Fiber Communication. OSA Technical Digest Series. Vol. 4* (OSA, Washington, D.C., 1993) pp 32–33.

7. Deri R.J., Pennings E.C.M., Scherer A., Gozdz A.S., Caneau C., Andreadakis N.C., Shah V., Curtis L., Hawkins R.J., Soole J.B.D., Song J.I. *Photon. Technol. Lett*., **4**, 1238 (1992).
8. Niemeier Th., Ulrich R. *Opt. Lett*., **11**, 677 (1986).
9. Pennings E.C.M., Deri R.J., Bhat R., Hayes T.R., Andreadakis N.C. *Proc. Eur. Conf. Opt. Commun.* (Genova, Italy, 1992) pp 461–464.
10. Christensen S.E., Koski O. In: *Advanced Solid-State Photonics. OSA Techn. Digest Series (CD)* (OSA, 2007) paper WC1.
11. Uberna R., Bratcher A., Alley T.G., Sanchez A.D., Flores A.S., Pulford B. *Opt. Express*, **18**, 13547 (2010).
12. Zhou P., Liu Z., Xu X., Chen Z. *Appl. Opt*., **47**, 3350 (2008).
13. Shay T.M., Baker J.T., Sanchez A.D., Robin C.A., Vergien C.L., Zerinque C., Gallant D., Lu C.A., Pulford B., Bronder T.J., Lucero A. *Proc. SPIE Int. Soc. Opt. Eng.*, **7195**, 71951M (2009).
14. Jolivet V., Bourdon P., Bennaï B., Lombard L., Goular D., Pourtal E., Canat G., Jaouën Y., Moreau B., Vasseur O. *IEEE J. Sel. Top. Quantum Electron*., **15**, 257 (2009).
15. Jianfeng Li, Kailiang Duan, Yishan Wang, Wei Zhao. *IEEE Photon. Technol. Lett*., **20**, 888 (2008).
16. Vorontsov M.A., Weyrauch T., Beresnev L.A., Carhart G.W., Liu L., Aschenbach K. *IEEE J. Sel. Top. Quantum Electron*., **15**, 269 (2009).
17. Yu C.X., Augst S.J., Redmond S.M., Goldizen K.C., Murphy D.V., Sanchez A., Fan T.Y. *Opt. Lett*., **36**, 2686 (2011).
18. Goodno G.D., McNaught S.J., Rothenberg J.E., McComb T.S., Thielen P.A., Wickham M.G., Weber M.E. *Opt. Lett*., **35**, 1542 (2010).
19. Ma Y., Wang X., Leng J., Xiao H., Dong X., Zhu J., Du W., Zhou P., Xu X., Si L., Liu Z., Zhao Y. *Opt. Lett*., **36**, 951 (2011).
20. Tao R., Si L., Ma Y., Zhou P., Liu Z. *Appl. Opt*., **51**, 5826 (2012).
21. Tao R., Wang X., Xiao H., Zhou P., Si L. *Photon. Res*., **1**, 186 (2013).
22. Nabors C.D. *Appl. Opt*., **33**, 2284 (1994).
23. Shellan J.B. *J. Opt. Soc. Am. A*, **2**, 555 (1985).
24. Goodno G.D., Chun-Ching Shih, Rothenberg J.E. *Opt. Express*, **18**, 25403 (2010).
25. Ulrich R., Kamiya T. *J. Opt. Soc. Am*., **68**, 583 (1978).
26. Bachmann M., Besse P.A., Melchior H. *Appl. Opt*., **33**, 3905 (1994).
27. He S., Ao X., Romanov V. *Appl. Opt*., **42**, 4855 (2003).
28. Scarmozzino R., Gopinath A., Pregla R., Helfert S. *J. Sel. Top. Quantum Electron*., **6**, 150 (2000).
29. Scarmozzino R., Osgood R.M. Jr. *J. Opt. Soc. Am. A*, **8**, 724 (1991).
30. Hadley G.R. *Opt. Lett*., **16**, 624 (1991).
31. Hadley G.R. *IEEE J. Quantum Electron*., **28**, 363 (1992).